Automated Identification of Buried Landmines Using Normalized Electromagnetic Induction Spectroscopy

Haoping Huang and I. J. Won

***Abstract*—Electromagnetic induction spectroscopy (EMIS) is used to identify a buried metallic object such as a landmine, based on its EMI spectrum. EMIS, however, depends on the object's electrical conductivity, magnetic permeability, shape, size, depth, and orientation. For a given mine made of specific metals, shape, and size, however, the only variables are the mine's burial depth and orientation. This paper describes a method of identifying a landmine using a normalized EMIS spectrum, which is independent of the orientation or depth. We assume that the target is small compared with its distance to or size of the sensor so that the source field at a target is uniform. In this case, the normalized spectrum will be range-independent and, therefore, the target identification is based on only spectral shapes. We have developed and tested an algorithm that matches a normalized EMIS spectrum to those of library targets. We applied the new process to 1) numerically simulated data, 2) experimental data from controlled sites using inert mines, mine simulants, and clutter items, and 3) finally extensive field data collected at a blind test site established by the U.S. Army. Test results show that targets are correctly identified with a misfit of less than 10%; they also show that 80% of clutter may be rejected, based on a misfit over 30%.**

***Index Terms*—Electromagnetic induction spectroscopy, identification, landmine, normalization.**

I. Introduction

ELECTROMAGNETIC induction spectroscopy (EMIS) is a promising new method of identifying a buried metallic object such as a landmine, based on its spectral response over a broad induction bandwidth [1], [2]. One of the outstanding issues is that most metal detectors can detect small metal pieces such as landmines, but cannot effectively discriminate a landmine amid ubiquitous false alarms in a cluttered environment. False alarms are anomalies caused by other metallic objects, soil heterogeneities, and other natural and cultural features. False alarms result in unnecessary excavations and, thus, significantly contribute to the cost of landmine clearance. A major research initiative, therefore, is to develop discrimination (target identification) capabilities.

EMIS response of a metal object depends on its conductivity, magnetic permeability, shape, size, orientation, and depth. Combinations of these factors may yield similar spectral responses for different targets. Even though the spectral response may not be unique for a target, the method can significantly reduce the number of false alarms and reject clutter. We describe in this paper a normalized EMIS response that can be used to identify a target.

Manuscript received July 5, 2001; revised November 24, 2002. This work was supported by the U.S. Army Night Vision Electronic Sensor Directorate (NVESD).

The authors are with Geophex, Ltd., Raleigh, NC 27603 USA.

Digital Object Identifier 10.1109/TGRS.2003.809937

Fig. 1. GEM-3 monostatic broadband EMI sensor.

II. EMIS Sensors

Broadband sensors suitable for the EMIS application are rather new and still in their commercial infancy. The GEM series developed by Geophex is one such group of sensors that are commercially available and have been used at many environmental sites, including those containing landmines and unexploded ordnance [1]–[8]. The GEM-3 sensor (Fig. 1), designed particularly for detecting small metallic targets, is used for the experimental results reported in this paper.

The GEM-3 operates in a bandwidth from 30 Hz–24 kHz. The sensing head consists of a pair of concentric, circular coils that transmit a continuous, broadband, digitally controlled, electromagnetic (EM) waveform. The two transmitter coils connected in an opposing polarity, with precise dimensions and placement, create a zone of magnetic cavity at the center of the two coils. A magnetic cavity is defined as a region where a directional sensor, placed in a specified orientation, produces zero signal induced from the magnetic field. The GEM-3's receiving coil is placed within this magnetic cavity so that it senses only the weak, secondary field returned from the earth and buried targets.

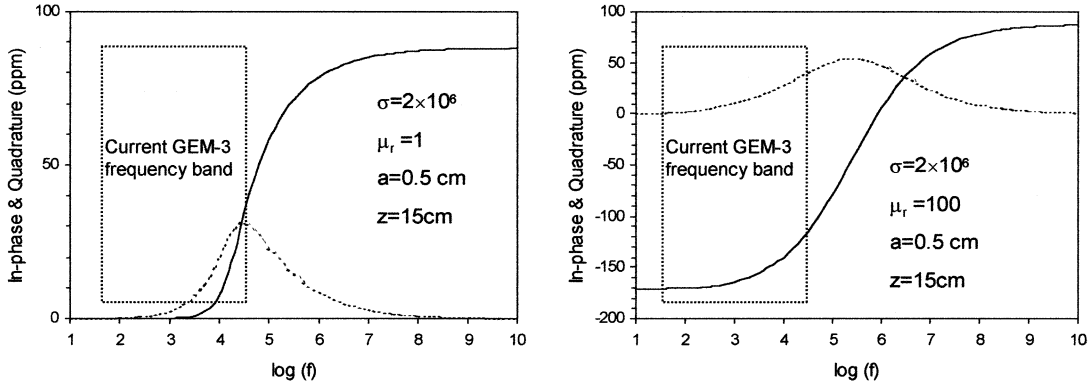

Fig. 2. Computed EMIS spectra of (a) nonpermeable and (b) permeable spheres with conductivity, relative permeability, radius, and depth as indicated. The rectangles show the current GEM-3 bandwidth. The solid lines stand for the in-phase, and the dotted lines for the quadrature (same for the remaining figures).

III. Electromagnetic Induction Spectroscopy

When an electrically conductive and/or magnetically permeable object is placed in a time-varying electromagnetic field, a system of induced current flows through the object. By observing a small secondary magnetic field emanating from the induced current, we attempt to detect the object; this is the foundation of the well-known electromagnetic induction (EMI) method. This method, however, cannot distinguish one metallic object from another, so the number of false targets generally far exceeds that of real targets. In other words, it detects metal objects indiscriminately and, thus, produces much wasted effort in excavating false targets. But by measuring the broadband spectrum of the secondary field, we obtain a distinct spectral signature that may identify the object. Based on the response spectrum, we can "fingerprint" the object. This is the basic concept of EMIS.

Although EMI physics is completely described by Maxwell's four equations, analytical solutions beyond the simplest geometry are rare. Thus, we have to obtain the spectral responses for most landmines by using physical modeling. Numerical modeling is easy and fast, but limited to the simplest geometry, such as a sphere, which is a useful model because small landmines often respond like a sphere. The EMI responses of a conductive and permeable sphere excited by a dipolar alternating magnetic field are given by Wait [9], [10], Grant and West [11], and Ward and Hohmann [12], among others. Fig. 2 shows the theoretical spectral responses of nonpermeable and permeable spheres. Available spectral bandwidth is dictated by hardware, and therefore, each sensor may have a different frequency window, as shown in Fig. 2. Obviously, the wider the window, the better the chance of identification.

A general approach for identifying a landmine, as well as for discriminating between landmines and clutter, is to match the EMIS spectrum measured above a target against signatures from known mines that are stored in a library. In a simple scenario, we first conduct a detection survey using multiple frequencies optimally chosen for a given geologic and cultural environment. Once a target is suspected (e.g., using audible tone), we place the sensor directly over the target (a spot of highest tonal output) and record the target's spectrum, which is then scanned through a spectral library for matching, in order to identify the target as a particular landmine or, if no match is found, to declare it as clutter. A given minefield would likely contain only a few types of mines at most, which would simplify the matching process.

IV. Normalized EMIS Spectrum

The EMI spectral response of an object is a function of its electrical conductivity, magnetic permeability, shape, size, depth, and orientation. For a specific landmine, however, its shape, size, conductivity, and permeability are given, leaving orientation and depth as the only variables. For the orientation issue, we may apply, given the depth, a preprocessing step that fits the data to a tensor dipole model, from which estimates of the target orientation are derived [13], [14]. Once this is done, the target can be effectively rotated into a principal axis coordinate system, and the spectral response in this system can be compared against those of library objects.

We do not consider the orientation issue a serious problem because common landmines have cylindrical symmetry and are laid flat for vertical pressure activation. Since the GEM-3 also has a cylindrical symmetry, the mutual view is fixed when the sensor is directly above the mine, and thus, the only factor left is depth with which the spectral response may vary.

Let us assume that the metal parts are small compared to the size of, or distance to, the sensor, so they can be treated as a point or a small sphere such that the source field at the point may be considered uniform. Large mines or clutters may be recognized from the audible tone. Then, the sensor can be raised at a proper height to make the primary field uniform at the target. Under this condition, a mine would produce the same spectral shape regardless of its distance to the sensor. To equalize the spectral shape, we normalize an EMIS spectrum by setting, for example, its highest in-phase value to one; in this way, the normalized EMIS spectra measured at various depths will be equal.

Table I shows properties of the landmine simulants used for our initial controlled experiments. These are surrogate mines without explosives and have been developed and manufactured by the U.S. Army as compositional representatives of all existing landmines, thus suitable for experiments related to mine detection and classification issues. As can be seen in Table I, some of the simulants consist of multiple metal parts that are

TABLE I
LANDMINE SIMULANTS AND THEIR METAL CONTENT AND SIZE. THE REST SHOWS EXPERIMENTALLY DETERMINED CONDUCTIVITY, RELATIVE PERMEABILITY, AND RADIUS OF AN EQUIVALENT SPHERE

Simulants	Metal Contents	Size (cm)	$\sigma\ 10^6$ (S/m)	μ_r	a (cm)
C_0	Carbon steel ball	0.32 D.	1.00	5.50	0.16
E_0	Carbon steel pin	0.69×0.16 D.	4.00	5.50	0.15
G_0	Copper tube	1.28×0.32 O.D.	12.48	1	0.29
I_0	Aluminum tube	1.28×0.48 O.D.	7.37	1	0.38
K_0	Aluminum tube+ E_0	1.28×0.64 O.D. 0.69×0.16 D.	4.67	1.53	0.47
M_0	Aluminum tube	3.84×0.64 O.D.	3.23	1	0.67
O_0	Steel pin+ M_0+ Carbon steel spring+ Carbon steel ball	1.38×0.16 D. 3.84×0.64 O.D. 2.56×0.88 0.64 D.	1.25	5.25	0.89

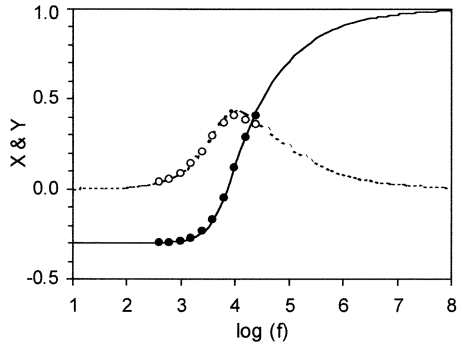

Fig. 3. Measured spectrum (circles) of a mine simulant K_0 is fit to the computed normalized spectrum (lines) to determine conductivity and permeability of an equivalent sphere. The solid circles stand for in-phase, and open circles for quadrature (same for the remaining figures).

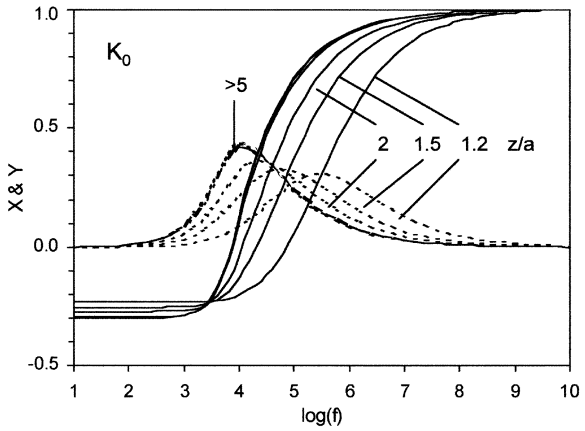

Fig. 4. Normalized EMIS spectra of a sphere, equivalent to K_0, as a function of its distance to the sensor. The maximum in-phase values are normalized to one.

close to each other, so that the assumption of a point or sphere model is satisfied. Otherwise, the sensor may be raised at a higher position to satisfy the assumption. We first experimentally determined the conductivity and magnetic permeability of each simulant by fitting its observed EMIS spectrum to the computed spectrum of an equivalent sphere. For example, Fig. 3 shows such a fit for K_0, a simulant consisting of a small aluminum tube and a carbon-steel pin. Because there is no simple solution for a cylinder for the current sensor geometry, we will use a sphere for numerical modeling for these mine simulators. The right-hand column in Table I presents volume-equivalent sphere radii of the simulants, all of which are smaller than 1 cm.

Fig. 4 depicts EMIS spectra of K_0 for several values of z/a, where z is the depth to the center of the sphere and a is the sphere radius. The spectral shape varies much when $z/a < 5$ due to near-field effects. When $z/a > 5$ or at far field, the spectra are virtually the same because the source field at the sphere is approximately uniform. For given conductivity and permeability, the spectral shape depends on z/a. The curves will shift to the lower frequency for a larger target and to the higher frequency for a smaller target. To meet the uniform source field condition for large targets, we may raise the sensor to increase z so as to keep $z/a > 5$.

As noted in Table I, all simulants have an equivalent radius less than 1 cm. Since the GEM-3 used for this study has an outer coil radius of 20 cm and, during a survey, the sensor is usually several centimeters above ground, we may assume that the source field is uniform across the target. For a given landmine, therefore, an amplitude-normalized spectral response would be independent of sensor height. Once a library of landmine signatures has been collected and stored, we proceed with the identification, using a process expressed as

$$\chi = \min\left\{\frac{\sum_{i=1}^{M}\left(\left|X_i - \hat{X}_i^j\right| + \left|Y_i - \hat{Y}_i^j\right|\right)}{\sum_{i=1}^{M}\left(\left|\hat{X}_i^j\right| + \left|\hat{Y}_i^j\right|\right)}\right\}, \quad j = 1, 2, \ldots, N \quad (1)$$

where χ is the misfit in percent; X_i and Y_i are the measured normalized in-phase and quadrature responses at ith frequency; $\hat{X}_i^j$ and $\hat{Y}_i^j$ are the normalized in-phase and quadrature in the library for ith frequency and jth landmine type; M is the number of frequencies; and N is the number of landmine types stored in the library. The measured spectrum is scanned through the library to find a best match. Then, according to the goodness of match, we may declare the object as a particular landmine or

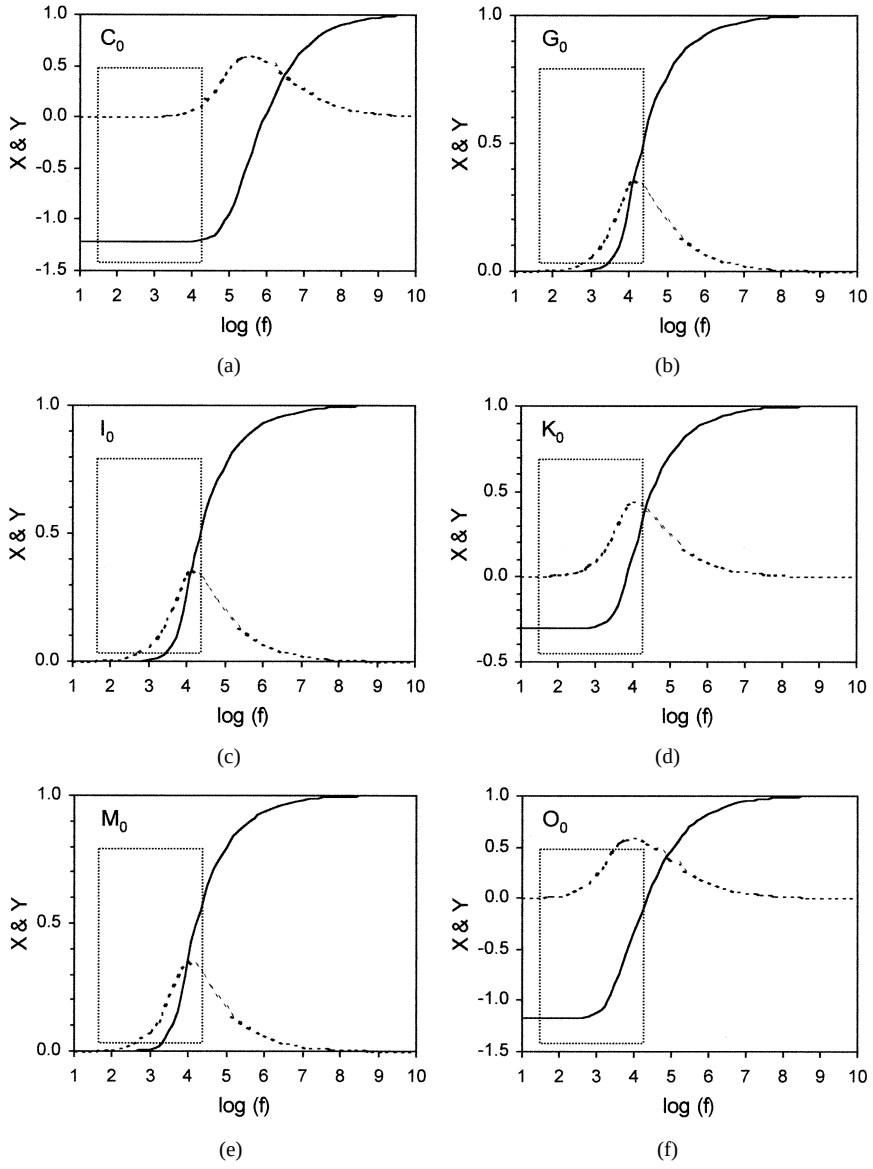

Fig. 5. Normalized EMIS spectra of six mine simulants, located at 10 cm from the GEM-3, using equivalent spheres as shown in Table I. Rectangles indicate the current GEM-3 bandwidth.

TABLE II
MATCH SCORES WHEN THE SIMULATED DATA ARE ADDED WITH NOISE OF 5% TO 70%. WHEN THE PROCESS CORRECTLY MATCHES A TARGET TO ITSELF, THE SCORE IS "1." WHEN IT PICKS ITSELF AS THE SECOND CHOICE, THE SCORE IS "2," ETC. NOTICE THAT FIVE OUT OF SEVEN ARE CORRECTLY IDENTIFIED EVEN WHEN THE NOISE LEVEL IS 70%

Target	5%	10%	15%	20%	30%	40%	50%	70%
C_0	1	1	1	1	1	1	1	1
E_0	1	1	1	1	1	1	1	1
G_0	1	1	2	2	3	3	3	3
I_0	1	1	1	2	2	2	2	2
K_0	1	1	1	1	1	1	1	1
M_0	1	1	1	1	1	1	1	1
O_0	1	1	1	1	1	1	1	1

reject the object as clutter. The declaration requires establishing a match threshold, perhaps for each mine separately, based on experiments. The criterion should err on the side of the caution so that the process, when not certain, sides with declaring an object as mine rather than as clutter.

TABLE III
MATCH SCORES WHEN THE DATA ARE ADDED WITH CONSTANTS OF 5% TO 70% OF THE IN-PHASE DATA AT THE HIGHEST FREQUENCY. SCORING METHOD IS THE SAME AS THAT IN TABLE II. THE DECIMAL NUMBERS IN THE RIGHT-HAND SUBCOLUMNS ARE THE MISFITS IN PERCENT

Target	5%		10%		15%		20%		30%		40%		50%		70%	
C_0	1	0.7	1	1.3	1	1.8	1	2.3	1	3.2	1	3.9	1	4.6	1	5.7
E_0	1	1.0	1	1.9	1	2.7	1	3.5	1	4.8	1	6.0	1	7.0	1	8.6
G_0	2	9.3	2	17.7	2	25.4	3	32.5	3	45.0	3	55.7	3	65.0	3	80.3
I_0	1	8.1	1	17.4	2	25.0	2	32.0	2	44.3	2	54.8	2	63.9	2	79.0
K_0	1	7.5	1	14.3	1	20.6	1	26.3	1	36.4	3	45.1	4	52.6	4	64.9
M_0	1	8.4	1	16.1	1	23.1	1	29.5	1	40.8	1	50.5	1	58.9	1	72.8
O_0	1	3.9	1	7.5	1	10.8	1	13.8	1	19.1	1	23.6	1	27.5	1	34.0

Absolute amplitude of the response is proportional to the total metal content and, therefore, an important indicator for the mine size. We define the total amplitude as

$$A = \sum_{i=1}^{M} (x_i^2 + y_i^2)^{1/2} \tag{2}$$

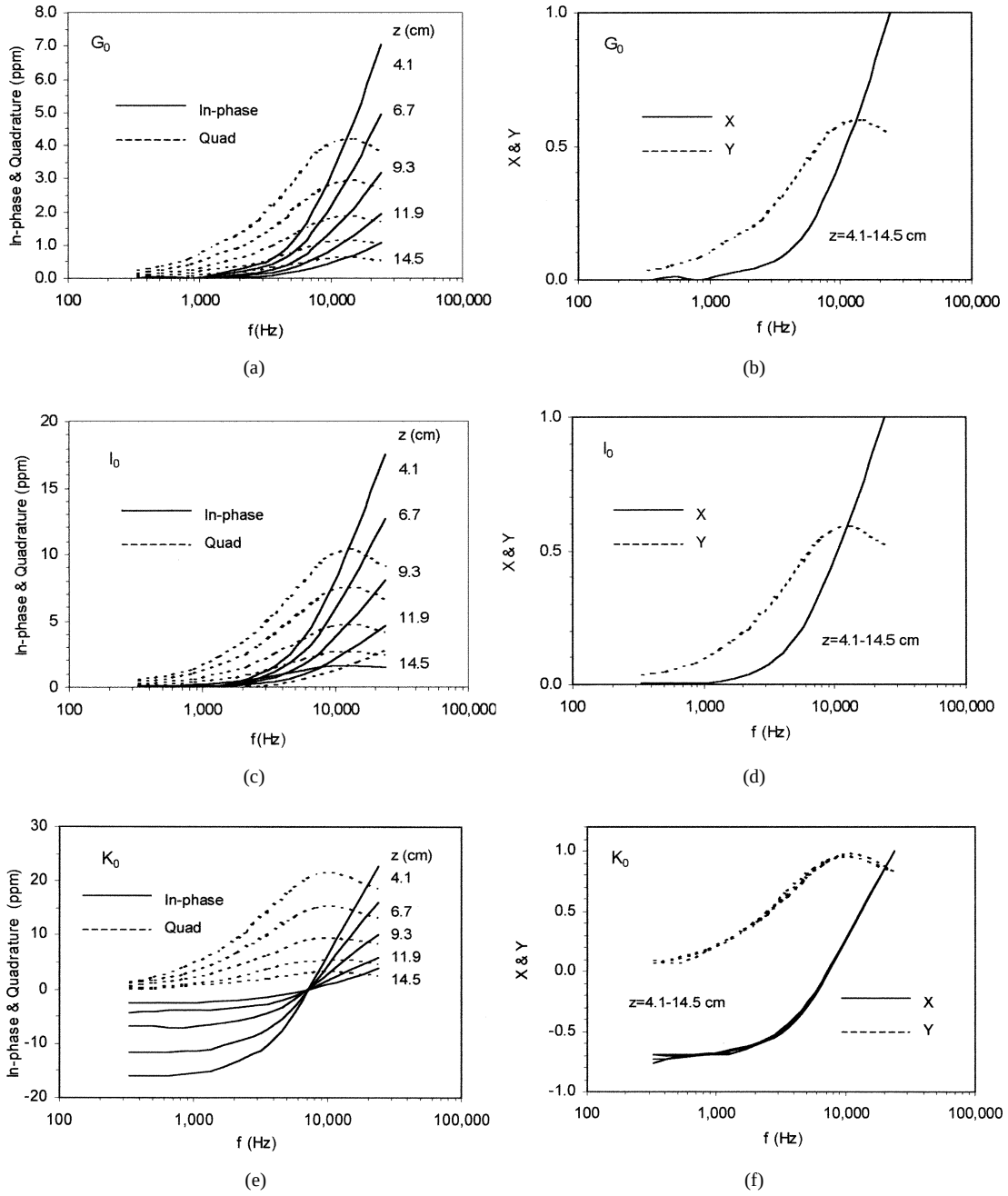

Fig. 6. Measured EMIS spectra (left) for five mine simulants G_0, I_0, K_0, M_0, and O_0 located at varying distances to the GEM-3 sensor and their corresponding normalized EMIS spectra (right).

where x_i and y_i are the observed in-phase and quadrature data at ith frequency. Thus, even when an observed spectrum matches well in shape with a library spectrum, the object may be declared clutter if the total amplitude is significantly wrong within an assumed depth range.

V. Numerical Simulations

We used a conductive and permeable sphere as a model, since it has an analytic solution [9]–[12]. The frequency bandwidth used in this study is from 10 Hz to 100 kHz. We first built a spectral library consisting of spheres equivalent in volume to the simulants listed in Table I. We then cross-matched the computed spectra by computing misfits among each other, based on (1).

Fig. 5 shows the normalized EMIS spectra for the simulants, except for E_0 whose spectrum is very similar to that of C_0. Mines with very small metal parts, such as C_0 and E_0, exhibit their spectral peaks higher than the current GEM-3 upper frequency limit. To detect and discriminate these mines, the bandwidth must be increased by one or two decades. Simulants G_0, I_0, and M_0 have similar spectral responses because the response parameter $(\sigma\mu\omega)^{1/2}a$ is very close for these targets. Therefore, it would be difficult to discriminate among

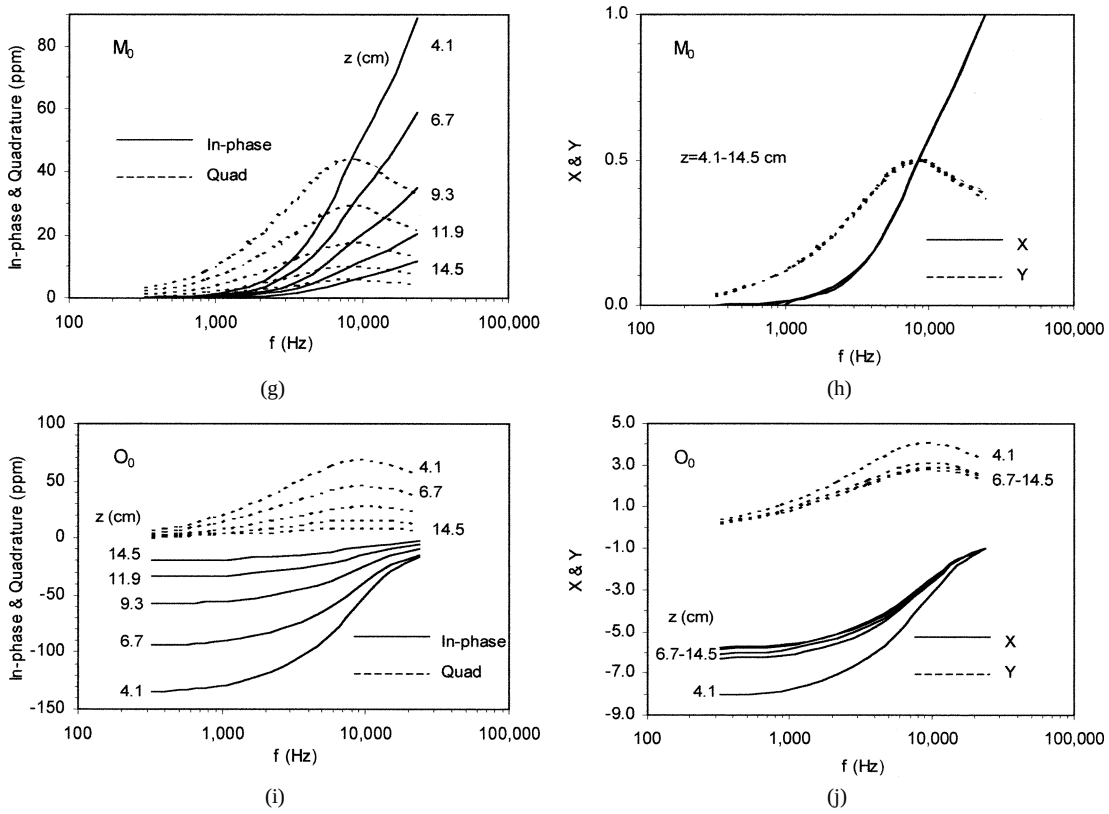

Fig. 6. *(Continued)* Measured EMIS spectra (left) for five mine simulants G_0, I_0, K_0, M_0, and O_0 located at varying distances to the GEM-3 sensor and their corresponding normalized EMIS spectra (right).

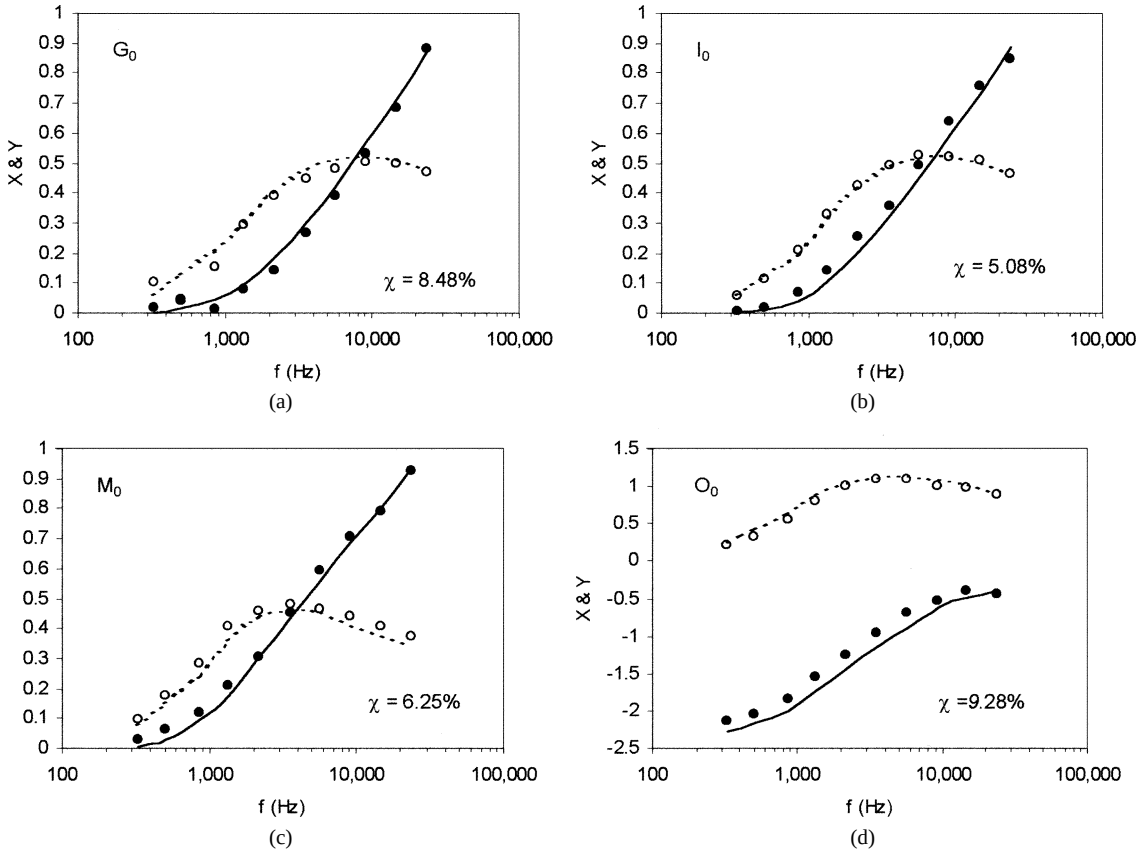

Fig. 7. Measured and normalized EMIS spectra (circles) of four mine simulants G_0, I_0, M_0, and O_0 buried in a hard clay ground, along with the best matching library spectra (lines) all of which are correctly identified.

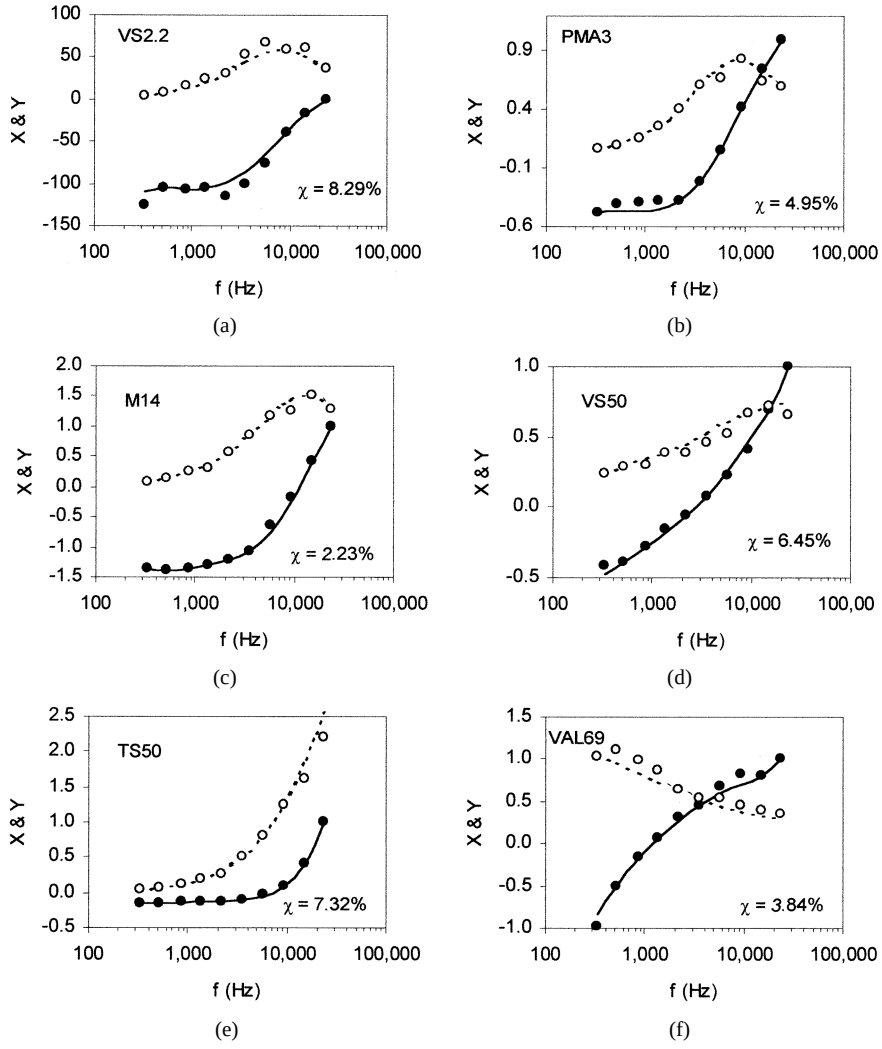

Fig. 8. Measured EMIS spectra (circles) obtained from six landmines, along with the best matching library landmine spectra (lines) all of which are correctly identified.

them in practice. However, M_0 is big in size so that amplitude of response will be high, which can be incorporated into the identification process.

To test the matching algorithm, we cross-matched the spectra computed for seven mine simulants and derive a misfit matrix using (1)

$$\chi = \begin{pmatrix} 0 & 18.41 & 89.83 & 89.92 & 80.77 & 91.90 & 52.59 \\ 18.71 & 0 & 75.61 & 75.71 & 65.94 & 77.95 & 36.07 \\ 145.61 & 120.59 & 0 & 0.17 & 19.45 & 3.85 & 77.75 \\ 145.62 & 120.63 & 0.17 & 0 & 19.53 & 3.68 & 77.78 \\ 115.81 & 93.04 & 17.21 & 17.30 & 0 & 19.20 & 51.57 \\ 145.69 & 121.59 & 3.76 & 3.60 & 21.23 & 0 & 78.25 \\ 55.25 & 37.29 & 50.40 & 50.47 & 37.79 & 51.86 & 0 \end{pmatrix}. \tag{3}$$

Here, the rows stand for the seven simulants (in the order of C_0, E_0, G_0, I_0, K_0, M_0, and O_0) in the library, and the columns are the same simulants in the same order, now used as unknown targets. Each diagonal element represents when a simulant is matched against itself, which results in a zero misfit for noise-free data, indicating that the match is perfect. Off-diagonals are misfits between two different simulants; for instance, χ_{16} (=91.90) is the misfit between C_0 and M_0. We note that the misfits for three nonferrous targets—G_0, I_0, and M_0—are small, as can be seen in χ_{34}, χ_{43}, χ_{36}, χ_{63}, χ_{46}, and χ_{64}, indicating that it would be difficult to discriminate among them. It is noted that the matrix is not symmetric as indicated by the denominator in (1).

We would not have a perfect match in the real world, so that a misfit threshold should be established for each mine. If the misfit is below the established threshold, we may accept the object as the corresponding landmine; otherwise, we declare it as clutter. In general, the threshold should be on the safe side so as to prevent a landmine from being classified as clutter. The threshold may vary depending on mine type, local geology, and cultural noise level of each minefield.

There are two major noise sources: random noise and geological background noise. For GEM-3 geometry, ground conductivity has little effects in the EM data when targets are metallic. Soil susceptibility, however, impacts greatly on the in-phase data, as observed over magnetic geology such as volcanic rocks (basalt, diabase, etc.) and lateritic soils (residual soil containing iron oxides and other magnetic minerals). In such places, the

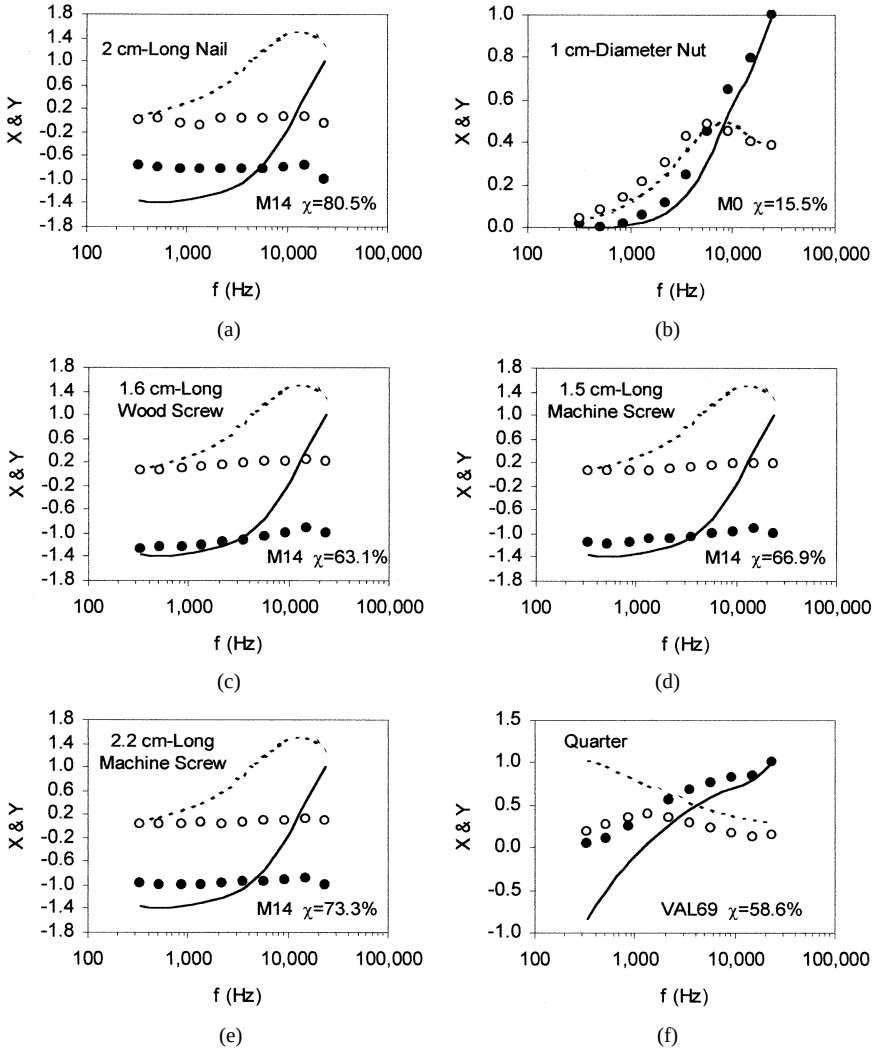

Fig. 9. Normalized spectra of selected clutter items (circles), along with the best matching library spectra (lines) shown in Figs. 7 and 8. It is obvious that majority of the clutter can be correctly rejected.

in-phase component becomes negative but constant at all frequencies and is sensitive to the sensor height. Therefore, the background noise comes from the variations in susceptibility and the sensor height. If the susceptibility or the sensor height varies rapidly from place to place, the spectrum will be distorted. For identification, we measure both the target and background spectra at the same sensor height for a few seconds, which are subtracted each other to remove the background response

We now assess the effect of noise by adding random noise to the data and deriving a misfit matrix similar to (3). Table II summarizes the identification scores for the added noise levels from 5% to 70%. The number in each cell denotes the rank of target selection: if the process selects the correct target as the first choice, the number is one, while if it selects the correct target as the second choice, the number is two, etc. All targets are correctly identified for noise levels up to 10%. Even at a 70% noise level, the process still correctly identifies five out of seven mines. The noise mainly affects the small nonferrous simulants G_0 and I_0. This is expected because their spectral responses are very similar to each other as shown in Fig. 5. Random noise appears to cause little impact on the results because the library is small, and the signatures are relatively distinct.

The effect of soil susceptibility is assessed by shifting the in-phase components by a constant and cross-matching the spectra for seven mine simulants. The constant is supposed to be the residual background. Table III summarizes the matching scores for the added constants from 5% to 70% of the in-phase data at the highest frequency. Again, the in-phase shift has a high impact on small nonferrous objects, G_0 and I_0, as indicated by their low scores even for a small shift. It should be noted that the score depends upon the items in the library, while the misfit depends upon the absolute value of the in-phase shift. These may explain the high score for O_0, whose spectrum is very different from the others and the added shifts may be small, since its in-phase value at the highest frequency is relatively small.

VI. Experimental Results

We then tested the identification process using a GEM-3 sensor, the mine simulants and inert mines. First, the assumption of uniform primary field should be proved. We placed a mine simulant in either air or soil and then measured the response at several heights above each target. Fig. 6 shows the

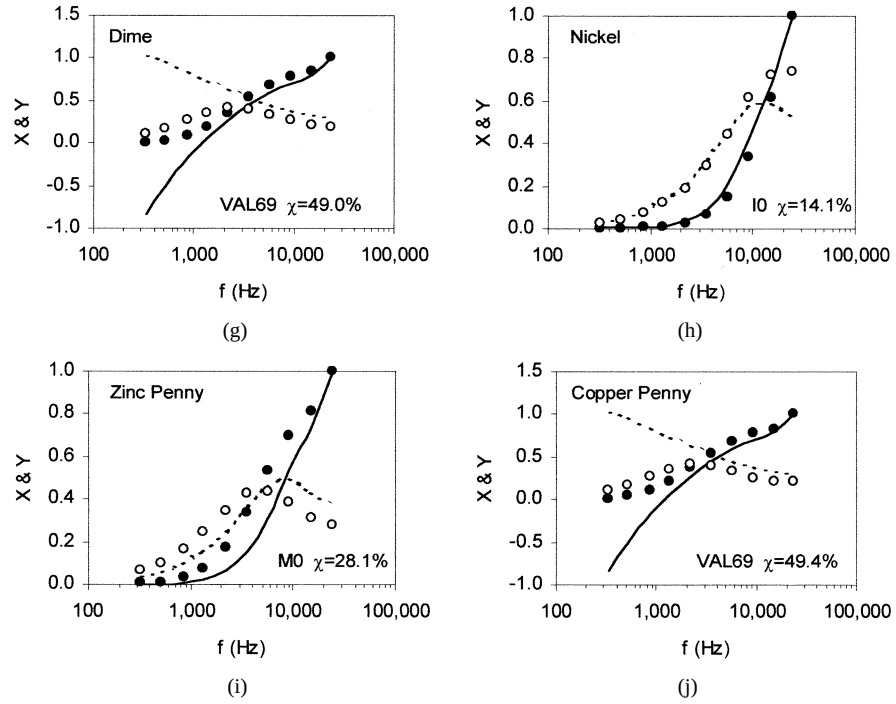

Fig. 9. *(Continued)* Normalized spectra of selected clutter items (circles), along with the best matching library spectra (lines) shown in Figs. 7 and 8. It is obvious that majority of the clutter can be correctly rejected.

observed (left) and normalized (right) spectra for simulants G_0, I_0, K_0, M_0, and O_0. The observed amplitude decreases as the distance increases. When normalized against the amplitude, however, the spectral shape becomes remarkably similar for all distances, indicating that the distance is nothing but a scale factor. This is not surprising because the GEM-3 transmitter coil with a radius of 20 cm can be treated as a large loop in comparison with much smaller landmines. Also note that Fig. 6, the actual GEM-3 data, compares favorably with Fig. 5, the computed spectra using a sphere model. We may choose any one of the heights in Fig. 6 as a library spectrum of a simulant.

Next, we tested the identification process by burying flush in the soil the simulants and several inert mines (i.e., all metal contents intact but without explosives). The library included eleven targets: five simulants, G_0, I_0, K_0, M_0, and O_0; a low-metal antitank (AT) mine VS2.2; and five antipersonnel (AP) mines, PMA3, M14, VS50, TS50, and VAL69. The GEM-3 data were acquired at ten simultaneous frequencies from 330 Hz to 23.970 kHz. Fig. 7 shows the normalized EMIS spectra of four simulants along with the best matched spectra in the library. Fig. 8 shows similar results for six inert mines. Note that all misfits are less than 10%.

When a target shows large misfits to all library mines, one may declare the target as clutter. When the misfit is not sufficiently large, however, the entire process is shaky at best. To illustrate this dilemma, Fig. 9 shows EMIS data obtained from ten clutter items (i.e., not mines) whose signatures are **not** included in the library. Each clutter is named on the upper left corner, while the best matched mine and misfit are indicated on the lower-right corner of each panel. It is obvious that the majority of the clutter shows very poor matches to any mines, so as to allow us to correctly declare them as clutter. Three items—the 1-cm-D nut, the U.S. nickel, and the U.S. zinc penny—match M_0 and I_0 with misfits of less than 30%. We may use the total amplitude A as shown in (2) to identify these objects further. For instance, the total amplitude of the nickel is much bigger than that of I_0 and, therefore, clutter. Total amplitudes of the other two items, however, have no significant difference from those stored in the library. Therefore, we do not have enough evidence to declare them as clutter. Thus, under a 30% misfit criterion, we can reject eight out of ten clutter items, or an 80% clutter rejection in this particular experiment, a significant reduction in false-alarm rate.

TABLE IV
LANDMINES BURIED IN THE BLIND GRIDS AT A U.S. ARMY TEST SITE. AT STANDS FOR ANTITANK MINE, AP FOR ANTIPERSONNEL MINE, M FOR LARGE METAL CONTENT, AND LM FOR LOW METAL CONTENT

Mine name	Type	Burial Depth
TM46	AT M	1-5 inches
VAL69	AP M	Surface-2 inches
M19	AT LM	1-5 inches
TMA4	AT LM	1-5 inches
VS2.2	AT LM	1-5 inches
TS50	AP LM	Surface-2 inches
VS50	AP LM	Surface-2 inches
PMA3	AP LM	Surface-2 inches
T72	AP LM	Surface-2 inches
TM62P3	AT LM	1-5 inches
M14	AP LM	Surface-2 inches

VII. DEMONSTRATION AT U.S. ARMY TEST SITE

The site consists of a small "calibration plot" containing identified landmines and a large blind test area that contains 980 test squares of 1×1 m. Each square may contain at the center a mine, clutter, or nothing. The calibration plot contains all mine types (see Table IV for the list) that are seeded in the blind grids.

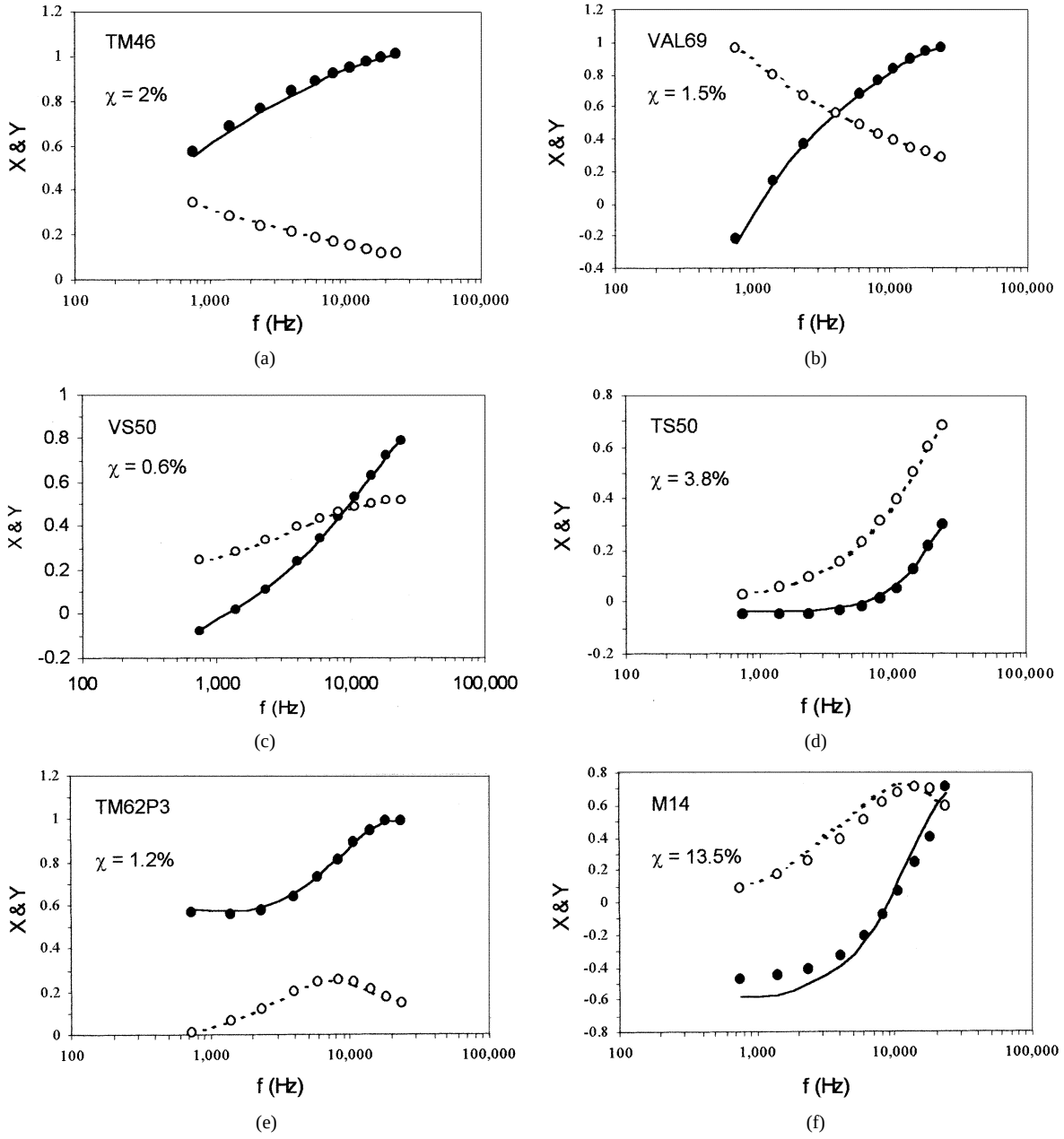

Fig. 10. Normalized EMIS spectra (circles) obtained from six blind grids at U.S. Army Test Site, along with the best matching library landmine spectra (lines). Each target was declared as the indicated best matching landmine.

We operated the GEM-3 at ten frequencies ranging from 750 Hz to 23.970 kHz. The EMIS library was made from the mines seeded in the calibration plot. Fig. 10 shows six example spectra obtained from the blind grids, along with their corresponding, best matching library spectra. Since all misfits are very low, and the total amplitudes of measured data are within the range of those of corresponding library spectra, we identify these targets with high confidence. The misfit threshold to declare a target as clutter depends on many factors, as we described earlier. Generally, the threshold should be inversely proportional to the target's metal content and proportional to its depth. The test indicated that the average misfit (ave) and its standard deviation (dev) are 2.5% and 0.6% for TM46, 2.7% and 1.4% for VAL69, 4.3% and 4.0% for VS50, and 17.8% and 10.2% for TS50. The figures would be higher as the metal content decreases.

Once we have established the misfit threshold for each mine, we may accept a target as a mine if the misfit between the two is less than ave + 2dev and reject it as clutter if greater than ave + 2dev. The M14 spectrum shown in the last panel of Fig. 10, for instance, matches the library M14 with a misfit of 13.5%, which would identify the target as M14 with high confidence because its average misfit could be higher than 20% in this case. In contrast, we declare the target Fig. 11(a) as clutter, since its misfit of 7.3% with its closest match, VAL69, is greater than ave + 2dev, even though the absolute value of the misfit is low. Likewise, the target in Fig. 11(b) matches to the T72 mine very well; however, the target's total amplitude is much higher than that for T72, and therefore, we confidently declare it as clutter.

For the test, we duplicated the data collection using two GEM-3 sensors, each by a different operator, in order to check

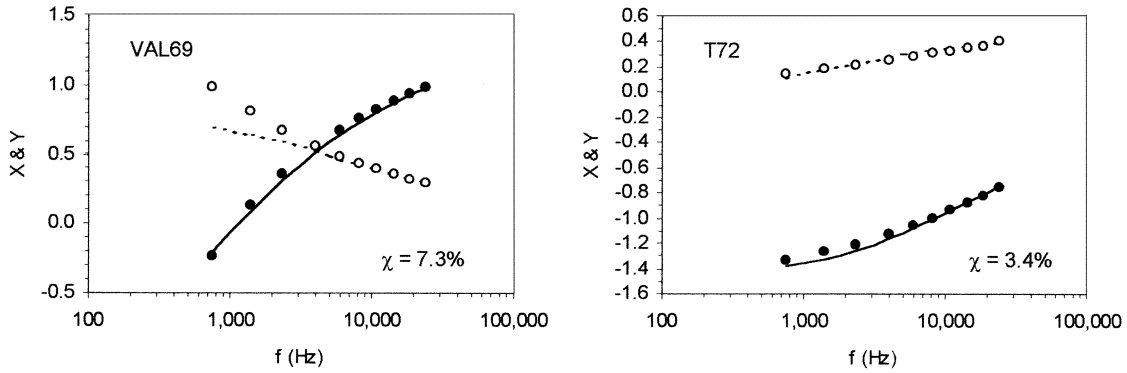

(a) (b)

Fig. 11. Normalized EMIS spectra (circles) obtained from two blind grids at U.S. Army Test Site, along with the best matching library landmine spectra (lines).

TABLE V
COMPARISON IN TARGET DECLARATION STATISTICS OF TWO GEM-3 SENSORS THAT WERE USED INDEPENDENTLY BY DIFFERENT OPERATORS AT U.S. ARMY TEST SITE

Mine Name	Quantity Declared	
	Sensor 6	Sensor 7
TM46	3	3
VAL69	5	5
TS50	35	35
VS50	10	10
Other LM	158	159
Clutter	769	768

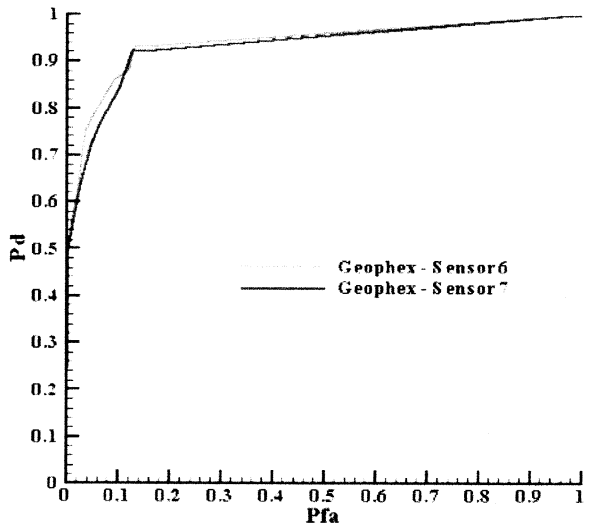

Fig. 12. ROC curves for two GEM-3 sensors showing their performance in terms of the PD and PFA based on the test result from U.S. Army Test Site.

the potential dependence on sensor or operator. Table V shows the number of mines declared by each sensor (labeled as Sensor 6 and Sensor 7), indicating a remarkable consistency in performance between the two sensors. Based on our test results (including detection, mine or not-mine declaration, and associated confidence level) from the blind test grids, the Night Vision Laboratory, the testing agency in this case, constructed the so-called receiver–operator characteristics (ROC) shown in Fig. 12. The x axis indicates the probability of false alarm (PFA), which is calculated by dividing the number of target declarations that are not truly targets by the total number of opportunities for false alarms; the y axis is the probability of detection (PD), which is the number of correct declarations divided by the number of target detection opportunities. The results from the two GEM-3 sensors are virtually the same, although the data have been collected and processed independently. The inflection point on the ROC curves indicates that, overall, we identified 92% of the landmines at a false-alarm rate of 12%.

Even though the PFA may seem acceptably small in this blind test, we need to understand the causes so that we may continue to improve the process. Some low-metal landmines, such as M19, may be easily misidentified because of their small metal content. We declared many more clutter as low-metal mines and vice versa. The signals from these low-metal mines are relatively low and, thus, are susceptible to various noises and requiring a high misfit threshold, which tends to produce erroneous results.

VIII. CONCLUSION

The normalized EMIS spectrum described here is based on the assumption that the primary magnetic field at a target is uniform. This assumption is valid for most types of landmines, since the targets' metal parts are small enough compared to the size and distance to the source. We have proved this assumption through theory, controlled tests, and an extensive blind test at a U.S. Army test site. The normalized spectrum eliminates the uncertain factor of depth. The normalized spectrum along with an associated amplitude threshold allows EMIS to be used in real time without requiring spatially distributed data. The concept is simple and practical.

In practice, an EMIS library should be developed preferably for each new minefield clearance operation. Starting with an empty library, we should conservatively excavate as many targets as practical in the beginning, store the spectrum before excavation, and, if the excavated item turned out to be a mine, add the spectrum into the mine library. This is a "learn-as-you-go" approach. Occasionally, a similar mine type may show different EMIS spectra, depending on manufacturer or batch; in that case, we would treat each as a different mine. On the other hand, the library should be kept as small as possible so as to simplify the identification process.

If an EMIS library includes all landmines occurring in a particular minefield, and if a target shows a large misfit in spec-

tral shape or in total amplitude, the target should be declared as clutter. A misfit threshold must be carefully established for each landmine based on local geology, clutter density, and cultural noise at a given minefield. According to our limited experiments, such a threshold may be specified as an average misfit plus two times standard deviation. Further research and experiments are needed to establish a firm ground for such thresholds. We also need to expand the sensor bandwidth, particularly to the high-frequency end, to detect and discriminate small, low-metal mines.

REFERENCES

[1] I. J. Won, D. A. Keiswetter, and E. Novikova, "Electromagnetic induction spectroscopy," *J. Environ. Eng. Geophys.*, vol. 3, no. 1, pp. 27–40, 1998.

[2] I. J. Won, D. A. Keiswetter, and T. H. Bell, "Electromagnetic induction spectroscopy for clearing landmines," *IEEE Trans. Geosci. Remote Sensing*, vol. 39, pp. 703–709, Apr. 2001.

[3] H. Huang and I. J. Won, "Conductivity and susceptibility mapping using broadband electromagnetic sensors," *J. Environ. Eng. Geophys.*, vol. 5, no. 4, pp. 31–41, 2000.

[4] D. A. Keiswetter, E. Novikova, I. J. Won, T. Hall, and D. Hanson, "Development of a monostatic, multifrequency electromagnetic mine detector," in *Soc. Opt. Eng.*, 1997, 3079, pp. 831–839.

[5] D. A. Keiswetter and I. J. Won, "Multifrequency electromagnetic signature of the Cloud Chamber, Nevada Test Site," *J. Environ. Eng. Geophys.*, vol. 2, no. 2, pp. 99–104, 1997.

[6] A. J. Witten and G. Calvert, "Characterizing the distribution of near-surface solution channels using electromagnetic induction and ground penetrating radar," *J. Environ. Eng. Geophys.*, vol. 4, no. 1, pp. 35–43, 1999.

[7] I. J. Won, D. A. Keiswetter, G. Fields, and L. Sutton, "GEM-2: A new multifrequency electromagnetic sensor," *J. Environ. Eng. Geophys.*, vol. 1, no. 2, pp. 129–137, 1996.

[8] I. J. Won, D. A. Keiswetter, D. Hanson, E. Novikova, and T. Hall, "GEM-3: A monostatic broadband electromagnetic induction sensor," *J. Environ. Eng. Geophys.*, vol. 2, no. 1, pp. 53–64, 1997.

[9] J. R. Wait, "A conducting permeable sphere in the presence of a coil carrying an oscillating current," *Can. J. Phys.*, vol. 31, pp. 670–678, 1953.

[10] ——, "On the electromagnetic response of a conducting sphere to a dipole field," *Geophysics*, vol. 25, pp. 619–658, 1960.

[11] F. S. Grant and G. F. West, *Interpretation Theory in Applied Geophysics*. New York: McGraw-Hill, 1965.

[12] S. H. Ward and G. W. Hohmann, "Electromagnetic theory for geophysical applications," in *Electromagnetic Methods in Applied Geophysics, Society of Exploration Geophysicists*, M. N. Nabighian, Ed., 1988, vol. 1, Theory, pp. 130–311.

[13] S. J. Norton and I. J. Won, "Identification of buried unexploded ordnance from broadband electromagnetic induction data," *IEEE Trans. Geosci. Remote Sensing*, vol. 39, pp. 2253–2261, Oct. 2001.

[14] S. J. Norton, I. J. Won, and E. R. Cespedes, "Ordnance/clutter discrimination based on target eigenvalue analysis," *Subsurface Sens. Tech. Appl.*, vol. 2, pp. 285–298, 2001.

Haoping Huang received the B.S. and M.S. degrees in geophysics from Changchun University of Earth Sciences, Changchun, China.

He is currently a Research Geophysicist at Geophex, Ltd., Raleigh, NC. He was a Professor of geophysics at Changchun University of Earth Sciences from 1982 to 1992. From 1987 to 1988, he was a Visiting Scholar at Brown University, Providence, RI. From 1993 to 1999, he was a Research Scientist at Geoterrex-Dighem, Toronto, ON, Canada. His current research focuses on electromagnetic methods in unexploded ordnance detection and discrimination. He has published numerous papers on airborne resistivity mapping, electromagnetic data processing, inversion, numerical modeling, digital signal processing, and other interpretation methods.

Mr. Huang is a member of the Society of Exploration Geophysics and the Australian Society of Exploration Geophysicists.

I. J. Won received the B.S. degree in mining engineering from Seoul National University, Seoul, Korea, in 1967, and the M.S. and Ph.D. degrees in geophysics from Columbia University, New York, in 1971 and 1973, respectively.

He is currently President of Geophex, Ltd., Raleigh, NC. From 1976 to 1989, he was Assistant Professor, Associate Professor, and Professor of geophysics at North Carolina State University, Raleigh. He has published over 100 research and review articles in journals and books.